Pairing theory for strongly correlated *d*-wave superconductors

Debmalya Chakraborty,[1,2] Nitin Kaushal,[1,3] and Amit Ghosal[1,*]

[1]*Indian Institute of Science Education and Research, Mohanpur, Kolkata 741246, India*

[2]*Institut de Physique Théorique, CEA-Saclay, Université Paris-Saclay, 91191 Gif-sur-Yvette, France*[†]

[3]*Department of Physics and Astronomy, The University of Tennessee, Knoxville, Tennessee 37996, USA*

(Received 7 August 2017; revised manuscript received 1 October 2017; published 24 October 2017)

Motivated by recent proposals of correlation induced insensitivity of *d*-wave superconductors to impurities, we develop a simple pairing theory for these systems for up to a moderate strength of disorder. Our description implements the key ideas of Anderson, originally proposed for disordered *s*-wave superconductors, but in addition takes care of the inherent strong electronic repulsion in these compounds, as well as disorder induced inhomogeneities. We first obtain the self-consistent one-particle states, which capture the effects of disorder exactly, and strong correlations using Gutzwiller approximation. These "normal states," representing the interplay of strong correlations and disorder, when coupled through pairing attractions following the path of Bardeen-Cooper-Schrieffer (BCS), produce results nearly identical to those from a more sophisticated inhomogeneous Hartree-Fock-Bogoliubov analysis that takes care of strong electronic repulsions.

DOI: 10.1103/PhysRevB.96.134518

I. INTRODUCTION

One of the outstanding puzzles of the disordered superconductors is the insensitivity of the high-temperature cuprate superconductors to weak and moderate disorder [1–5]. In contrast, the conventional wisdom developed along the lines of Abrikosov-Gorkov (AG) theory [6] predicts an extreme sensitivity of these materials to impurities. The original idea, based on perturbative expansions, had been refined subsequently, leading to self-consistent T-matrix calculations [7–12], but the broad sensitivity [13] of these materials to disorder survived.

The effects of dopant disorder [14], however, on cuprates have remained rather benign. The inhomogeneities in local doping of the charge carrier induce local variations in the gap map seen from the scanning tunneling microscopy measurements [15–17]. Surprisingly, these nanoscale inhomogeneities do not affect the low-energy density of states—as if the *d*-wave nodes are "quantum protected" [18]. The superfluid density and T_c undergo only modest reductions [19–21] in spite of the *d*-wave nature of the anisotropic order parameter [22–25]. Other unconventional superconductors, e.g., organics [26] and pnictides [27,28], which belong to the intermediate coupling category, also feature anomalies. On the other hand, addition of strong substitutional impurities [4,29] in these materials weakens superconducting correlations significantly.

A number of non-BCS features of high-T_c cuprate superconductors [30–32] make them deviate from a favorable playground of AG-type theories. These include the presence of strong repulsive correlations between the charge carriers, short coherence lengths, ξ, nonmonotonic dependence of T_c on the doping level, small superfluid density, etc. In addition, neglect of the spatial fluctuations in the pairing amplitude in a disordered environment in AG formalism calls for a careful microscopic re-examination of the role of impurities on these systems.

Inclusion of the spatial inhomogeneities of the pairing amplitude for short-coherence length *d*-wave BCS superconductors (dSC) within a Bogoliubov-de Gennes (BdG) formalism indeed enhances the robustness of dSC to impurities [33–36]. Recent advances of incorporating the effects of strong electronic repulsions on top of the inhomogeneous background resulted in a Gutzwiller-renormalized theory [5,37–39] (referred to as GIMT). These analyses make these superconductors amazingly immune to disorder, up to its strength as large as the bandwidth [40]! Such remarkable robustness of the superconducting correlations [5,40–42] naturally implies a similar robustness of T_c, at least within the mean-field description of the renormalized theory. This raises an intrinsic question: does Anderson's theorem [43], or an equivalent one, apply even for these strongly correlated *d*-wave superconductors?

We address this question by exploring the fate of a simple-minded pairing theory following Anderson's original idea of "pairing of exact eigenstates" [43,44]. But we upgrade it now to include the inherent strong correlations in these systems, as well as the exact treatment of disorder-induced inhomogeneities in our numerical calculations. It is well established that the "pairing of exact eigenstates" leads to Anderson's theorem for *s*-wave superconductors (sSC) for weak disorder. However, the same ideas had been successfully extended for sSC to incorporate details of inhomogeneities and localization effects in its numerical implementation [44] (see also Ref. [45]). Here, we expand it further by implementing similar concepts for strongly correlated superconductors with an anisotropic order parameter.

At the outset, we emphasize that our developments pertain to dSC with impurities up to a moderate strength and exclude strong substitutional scatterers. Studies of dSC with strong substitutional impurities, in the limit of unitary scatterers are also available [4,20,29,46,47]. There are subtleties in handling strong correlations and also strong impurities in a mean-field formalism [48], and the results depend crucially on their relative strengths.

In this article, we demonstrate that the complexity of strongly correlated disordered superconductors, such as

*Corresponding author: ghosal@iiserkol.ac.in

†Present address.

cuprates, can be understood in terms of a simple pairing theory. However, the true potential of our developments lies in identifying the underlying *exact quasiparticle states* in these strongly correlated and disordered systems, which we termed as the "normal states" (NS). It is these states that participate in Cooper pairing in these materials following the standard BCS path [49]. We posit that the properties of the true normal state dictate the response of anisotropic superconductors to impurities, providing a deeper insight to the physics of strongly correlated unconventional superconductors.

II. MODEL AND METHODS

A. Anderson's prescription

The original proposition of the pairing of exact eigenstates, which leads to Anderson's theorem, relies on two important conceptual ideas: (a) the problem of *noninteracting* electrons in disorder potential is solved at the first stage to generate its "exact eigenstates." BCS-type attractive pairing interactions then couple specific pairs of these states producing Cooper pairs at the second stage and the phase coherence of these pairs produces superconductivity in the disordered background. We emphasize that such decoupling of these two stages in the above mechanism necessarily demands that the pairing interactions have no role in determining the exact eigenstates. (b) The specific states participating in Cooper pairing (at the second stage) are the time reversed exact eigenstates derived in the first stage. This is simply motivated by the BCS theory, which Anderson's pairing method must reduce to, in the clean limit.

Each of these two points are important for establishing Anderson's theorem for disordered sSC. Can they work for the strongly correlated d-wave superconductors as well? In order to explore this question, we first set up the formalism below.

B. Normal states: "exact quasiparticle states" of a strongly correlated disordered system

In the limit when the electron-electron repulsion is strong, it is believed that the phases of the strongly correlated cuprates are driven by effective exchange interactions [50], and are formally described by the "t-J'' model [51]:

$$\mathcal{H}_{\text{t-J}} = \sum_{ij\sigma} t_{ij}\left(\tilde{c}^{\dagger}_{i\sigma}\tilde{c}_{j\sigma} + \text{H.c.}\right) + \sum_{ij} J_{ij}\left(\tilde{\mathbf{S}}_i.\tilde{\mathbf{S}}_j - \frac{\tilde{n}_i\tilde{n}_j}{4}\right). \tag{1}$$

The first term indicates hopping of electrons on a $2D$ square lattice of N sites. Here, J is the exchange interaction, assumed to arise from a Hubbard-type [52] on-site repulsion U via modified Schrieffer-Wolff transformation as implemented in Refs. [53,54], yielding $J_{ij} = 4t^2_{ij}/U$. We take $t_{ij} = -t$, when i and j are nearest neighbors, denoted as $\langle ij\rangle$, and $t_{ij} = t'$, when i and j are next-nearest neighbors, with the notation of $\langle\langle ij\rangle\rangle$. We choose $t_{ij} = 0$ for all other pairs of i and j. Correspondingly, we have $J_{ij} = J$ for $\langle ij\rangle$, $J_{ij} = J'$ for $\langle\langle ij\rangle\rangle$. Here, $\tilde{c}_{i\sigma} = c_{i\sigma}(1 - n_{i\bar{\sigma}})$ is the electron annihilation operator in the "projected Hilbert space" that prohibits double-occupancy at any site i, and similarly for the electron creation operator. We introduce disorder by redefining $\mathcal{H}_{\text{t-J}}$ to $\mathcal{H}_{\text{t-J}} + \sum_{i\sigma}(V_i - \mu)n_{i\sigma}$, where μ is the chemical potential that fixes the average density of electrons, $\rho = N^{-1}\sum_{i\sigma}\langle n_{i\sigma}\rangle$, in the system to a desired value. Such a simple re-definition of the Hamiltonian upon inclusion of disorder, however, would not work for strong disorder ($V \geqslant 3t$) and a revised treatment of Schrieffer-Wolff transformation [48,55,56] is necessary. Here, we use the model of *Box-disorder*, where V_i's on all sites i of the lattice are drawn from a uniform "box" distribution, such that, $V_i \in [-V/2, V/2]$ uniformly, thus defining V as the strength of disorder.

We studied the Hamiltonian $\mathcal{H}_{\text{t-J}}$ at zero temperature ($T = 0$), upon including disorder, over a wide range of parameters. Here we present results for $U = 12t$ and $t' = t/4$ [57], and we express all energies in the units of t. We choose the average density of electrons, $\rho = 0.8$, which coincides with the optimal doping. It is the optimal doping where dSC is the strongest in a typical phase diagram of cuprates, in addition to being reasonably free from the complex effects of other competing orders [38,58–63]. While the phenomenology of competing orders attract interesting and active research in the underdoped regime [64–68], our goal here is to focus only on the interplay of impurities and strongly correlated dSC, and hence we choose the optimal doping for our study. We carry out our numerical simulations typically on a 30×30 lattice, and we collect statistics on our results for each disorder strength V from 10–15 independent realizations of disorder.

The Hilbert space restriction, that prohibits any double occupancy in the limit of strong correlations, are reflected in the transformation: $c_{i\sigma} \to \tilde{c}_{i\sigma}$, and makes it difficult to handle these creation and annihilation operators in the projected space. To make progress, we use Gutzwiller approximation (GA) [37,69,70] to implement the phase space restrictions. GA amounts to renormalizing the parameters t and J of $\mathcal{H}_{\text{t-J}}$ locally by density-dependent factors, such that, they mimic the projection due to strong repulsions. For example, the restricted hopping reduces t_{ij} due to double-occupancy prohibition, whereas, the effective J_{ij} increases because of enhanced overall single occupancy. The real advantage of GA lies in the fact that it turns the problem into an effective weak coupling one redefined in the unprojected Hilbert space, which is now amenable to simple mean field treatments. It has been shown that GA is capable of describing non-BCS and nontrivial features of cuprate superconductors [71,72] in the clean limit (see however, Ref. [73]).

Upon carrying out the inhomogeneous Hartree-Fock mean field decoupling of the Gutzwiller renormalized $\mathcal{H}_{\text{t-J}}$ such that *no symmetry of* $\mathcal{H}_{\text{t-J}}$ *is broken*, we arrive at the following normal-state Hamiltonian:

$$\mathcal{H}_{\text{NS}} = \sum_{i,\delta,\sigma}\left(t_{i\delta}g^{t}_{i,i+\delta} - W^{\text{FS}}_{i\delta}\right)c^{\dagger}_{i\sigma}c_{i+\delta\sigma} + \sum_{i,\tilde{\delta},\sigma}\left(t_{i\tilde{\delta}}g^{t}_{i,i+\tilde{\delta}}\right)c^{\dagger}_{i\sigma}c_{i+\tilde{\delta}\sigma} + \sum_{i,\sigma}\left(V_i - \mu + \mu^{\text{HS}}_i\right)n_{i\sigma}. \tag{2}$$

Here, we have written the Hamiltonian on bonds connecting sites i and j, where $j = i + \delta$, with $\delta = \pm x$ or $\pm y$, $\tilde{\delta} = \pm(x \pm y)$. As the name suggests, we refer to the eigenstates of $\mathcal{H}_{\text{NS}}$ in Eq. (2) as the normal states, NS_{GIMT} (here, GIMT

in the subscript of normal states, NS, stands for Gutzwiller-augmented inhomogeneous Hartree-Fock mean-field theory). It is crucial to include the effect of strong correlations in $\mathcal{H}_{\rm NS}$ following the above construction, even though the final one-particle Hamiltonian without broken symmetries is similar in structure to the disordered tight binding model (or Anderson model of disorder). Yet, these normal states distinguish themselves from the "exact eigenstates" (eigenstates of the Anderson model of disorder) in accounting for the strong correlation effects through Gutzwiller factors, as well as the Hartree and Fock shifts. These considerations naturally make the solution of $\mathcal{H}_{\rm NS}$ already a self-consistent problem. We also emphasize that these normal states are defined at $T = 0$, and are not to be confused with the common notion of the high-temperature normal state of the material in which thermal fluctuations destroy superconductivity. The Fock-shift ($W_{i\delta}^{\rm FS}$) and the Hartree-shift ($\mu_i^{\rm HS}$) terms in Eq. (2) are given by

$$W_{i\delta}^{\rm FS} = \frac{J}{2}\left[\left(\frac{3g_{i,i+\delta}^{xy}}{2} - \frac{1}{2}\right)\tau_i^{\delta}\right], \tag{3}$$

$$\mu_i^{\rm HS} = -4t\sum_{\delta,\sigma}\left(\frac{\partial g_{i,i+\delta}^{t}}{\partial\rho_i}\tau_i^{\delta}\right) + 4t'\sum_{\tilde{\delta},\sigma}\left(\frac{\partial g_{i,i+\tilde{\delta}}^{t}}{\partial\rho_i}\tau_i^{\tilde{\delta}}\right) - \frac{3J}{2}\sum_{\delta,\sigma}\frac{\partial g_{i,i+\delta}^{xy}}{\partial\rho_i}\left(\tau_i^{\delta^2}\right), \tag{4}$$

where $\rho_i = \sum_\sigma \langle n_{i\sigma}\rangle_0$ and $\tau_{ij} \equiv \langle c_{i\downarrow}^\dagger c_{j\downarrow}\rangle_0 \equiv \langle c_{i\uparrow}^\dagger c_{j\uparrow}\rangle_0$. Here, $\langle\rangle_0$ denotes the expectation value in the unprojected space. The Gutzwiller factors in Eqs. (3) and (4) are given in terms of the local density:

$$g_{ij}^{t} = \sqrt{\frac{4(1-\rho_i)(1-\rho_j)}{(2-\rho_i)(2-\rho_j)}}, \quad g_{ij}^{xy} = \frac{4}{(2-\rho_i)(2-\rho_j)}. \tag{5}$$

As mentioned, the above construction of the $\rm NS_{GIMT}$ excludes any broken symmetry order parameters, e.g. magnetism, charge density wave, etc. However, unbroken symmetry is not a fundamental requirement of $\rm NS_{GIMT}$. In fact, we need to include them in $\mathcal{H}_{\rm NS}$ (except, of course, any superconducting order through Bogoliubov channels), when we study the effects of such additional orders competing with superconductivity.

Considering the unitary transformation to diagonalize $\mathcal{H}_{\rm NS}$ in the $\{\alpha\}$ basis:

$$c_{i\sigma} = \sum_{\alpha=1}^{N}\psi_i^{\alpha}c_{\alpha\sigma}, \tag{6}$$

we obtain $\mathcal{H}_{\rm NS} = \sum_{\alpha,\sigma}\xi_\alpha c_{\alpha\sigma}^\dagger c_{\alpha\sigma}$. Here, the self-consistent $\{\psi_i^\alpha\}$ are the eigenvectors of $\mathcal{H}_{\rm NS}$, and they constitute our "normal states", i.e., the $\rm NS_{GIMT}$.

C. Pairing of normal states (PNS)

To study the superconducting properties of $\mathcal{H}_{\rm t-J}$ in Eq. (1), we now introduce the pairing term in real-space representation,

$$\mathcal{H}_{\rm P} = \frac{1}{2}\sum_{\langle ij\rangle}\Delta_{ij}(c_{i\uparrow}^\dagger c_{j\downarrow}^\dagger - c_{i\downarrow}^\dagger c_{j\uparrow}^\dagger) + \text{H.c.} \tag{7}$$

in addition to $\mathcal{H}_{\rm NS}$, where

$$\Delta_{ij} = -\frac{J}{2}\left(\frac{3g_{ij}^{xy}+1}{4}\right)(\langle c_{i\uparrow}c_{j\downarrow}\rangle_0 - \langle c_{i\downarrow}c_{j\uparrow}\rangle_0). \tag{8}$$

The pairing part of the Hamiltonian in Eq. (7) can be thought to arise from a mean-field decoupling of the original $\mathcal{H}_{\rm t-J}$ in the Bogoliubov channel. Note that the form of $\mathcal{H}_{\rm P}$ ensures that we have chosen the singlet pairing channel on the links. Writing $H_{\mathcal{P}}$ in the $\{\alpha\}$ basis, we have,

$$\mathcal{H}_{\rm P} = \frac{1}{2}\sum_{\alpha\beta}\Delta_{\alpha\beta}(c_{\alpha\uparrow}^\dagger c_{\beta\downarrow}^\dagger - c_{\alpha\downarrow}^\dagger c_{\beta\uparrow}^\dagger) + \text{H.c.}, \tag{9}$$

where

$$\Delta_{\alpha\beta} = \sum_{\langle ij\rangle}\Delta_{ij}\left(\psi_i^\alpha\right)^*\left(\psi_j^\beta\right)^*, \tag{10}$$

leaving the total Hamiltonian as

$$\mathcal{H}_{\rm total} = \sum_{\alpha,\sigma}(\xi_\alpha - \mu_p)c_{\alpha\sigma}^\dagger c_{\alpha\sigma} + \frac{1}{2}\sum_{\alpha\beta}[\Delta_{\alpha\beta}(c_{\alpha\uparrow}^\dagger c_{\beta\downarrow}^\dagger - c_{\alpha\downarrow}^\dagger c_{\beta\uparrow}^\dagger) + \text{H.c.}]. \tag{11}$$

Here, we introduced μ_p to fix the final average density (after pairing) to the desired value $\rho = 0.8$. Note that the μ in $\mathcal{H}_{\rm NS}$ fixes the density to the same desired value, but only in the normal state. Pairing at the second stage (after inclusion of $\mathcal{H}_{\rm P}$) can deviate ρ from this value. We use μ_p to tune it back to the chosen value. We also note that there is no restriction, in principle, on α, β in the definition of $\Delta_{\alpha\beta}$ appearing in Eq. (10), though we will see in Sec. III E that the dominant contribution comes from those α, β for which $\xi_\alpha \approx \xi_\beta$.

D. Self-consistent pairing amplitude

Evidently, $\mathcal{H}_{\rm total}$ in Eq. (11) carries the BCS structure, however, our $\mathcal{H}_{\rm P}$ in the real space ensures that the disorder induced spatial information is included in $\Delta_{\alpha\beta}$ through the normal-state wave functions in Eq. (10). Next, we diagonalize it using a modified Bogoliubov transformation:

$$c_{p\sigma} = \sum_{n=1}^{N}(u_{p,n}\gamma_{n\sigma} - \sigma v_{p,n}^*\gamma_{n\bar{\sigma}}^\dagger), \tag{12}$$

where $\gamma_{n\sigma}^\dagger$ ($\gamma_{n\sigma}$) are fermionic quasiparticle creation (annihilation) operators.

Starting with guess values of Δ_{ij} on all the $2N$ bonds, we first obtain the N^2 numbers of $\Delta_{\alpha\beta}$ using the normal state eigenfunctions ψ_i^α's in Eq. (10). The eigenvalues and eigenvectors of $\mathcal{H}_{\rm total}$ allow us to recalculate Δ_{ij} and ρ_i using Eq. (8) and the self-consistency conditions (see Ref. [74] for details):

$$\langle c_{i\uparrow}c_{j\downarrow}\rangle_0 = \sum_{p_1,p_2=1}^{N}\psi_i^{p_1}\psi_j^{p_2}\langle c_{p_1\uparrow}c_{p_2\downarrow}\rangle, \tag{13}$$

$$\rho_i = 2\sum_{p_1,p_2=1}^{N}\left(\psi_i^{p_1}\right)^*\psi_i^{p_2}\langle c_{p_1\downarrow}^\dagger c_{p_2\downarrow}\rangle. \tag{14}$$

We then iteratively update the guess values of Δ_{ij} and ρ_i for the inputs in Eq. (11) in order to achieve the final self-consistency until the inputs and corresponding outputs in Eq. (13) and (14) match within tolerance. For accelerating the convergence, we used combinations of linear, Broyden and modified Broyden [75] schemes of mixing of the input and output at every iteration.

III. RESULTS

We will discuss in this section our findings from the pairing of normal states (PNS) and compare them with GIMT findings. Here, GIMT refers to the full BdG calculation augmented with Gutzwiller renormalization. However, it is truly illuminating to focus our attention first on the distinguishing features of $\mathrm{NS_{GIMT}}$ that separate them from their uncorrelated counterparts—the "exact eigenstates" of the Anderson's model of disorder.

A. Structure of the *normal states*

For the convenience of our discussions below, it is useful to cast the normal-state Hamiltonian $\mathcal{H}_{\mathrm{NS}}$ in the following form:

$$\mathcal{H}_{\mathrm{NS}} = -\sum_{i,\delta,\sigma} t_{\mathrm{eff}}(i,\delta) c^{\dagger}_{i,\sigma} c_{i+\delta,\sigma} + \sum_{i,\sigma} V_{\mathrm{eff}}(i) n_{i,\sigma}, \qquad (15)$$

to emphasize $\mathcal{H}_{\mathrm{NS}}$ as a tight-binding model, but with effective disorder *both* on the links (t_{eff}) and on the sites (V_{eff}). However, these disorder terms now contain order parameters, as seen from Eqs. (2)–(4), and hence, must be evaluated self-consistently, as mentioned already. We find them to develop spatially correlated structures [74], and are illustrated in Figs. 1(a)–1(d). For a justified comparison between the spatial structures of V_{eff} and t_{eff}, we transformed the bond variable $t_{\mathrm{eff}}(i,\delta)$ to a site variable using the relation $t_{\mathrm{eff}}(i) = \frac{1}{4}\sum_{\delta} t_{\mathrm{eff}}(i,\delta)$. Spatial associations are found, firstly, in the profile of $V_{\mathrm{eff}}(i)$ itself, showing conglomeration of regions with large and small V_{eff}, but more importantly, through the explicit anticorrelation of regions of V_{eff} and t_{eff} in space. We also compare the distributions $P(V_{\mathrm{eff}})$ and $P(t_{\mathrm{eff}})$ for $V = 1.75$ from the $\mathrm{NS_{GIMT}}$ and GIMT results in Figs. 1(e) and 1(f), using statistics over ten realizations of disorder. Such a favorable comparison of $\mathrm{NS_{GIMT}}$ outputs of t_{eff} and V_{eff} with those from GIMT validates the conceptual basis of the PNS formalism. The role of strong electronic repulsions on the disordered normal states has a simple and intuitive rationale, as we describe below. A random impurity potential tends to generate charge inhomogeneities in space, whereas, repulsive interactions smear out such heterogeneities, trying to restore its homogeneous distribution. The key ingredient of $\mathrm{NS_{GIMT}}$ that distinguishes it from the exact eigenstates lies in its impurity renormalization—a footprint of electronic repulsion in $\mathrm{NS_{GIMT}}$. This is ascribed to the modification the hopping amplitudes based on local density, which smear out charge accumulation near deep potential wells, and also partly populating potential hills, as explained in Fig. 2. As a schematic description, we consider in Fig. 2 a site i having a high hill of local potential, and hence it ordinarily supports little density of electrons there, compared to the average density on its neighbors, assumed to have no disorder. This

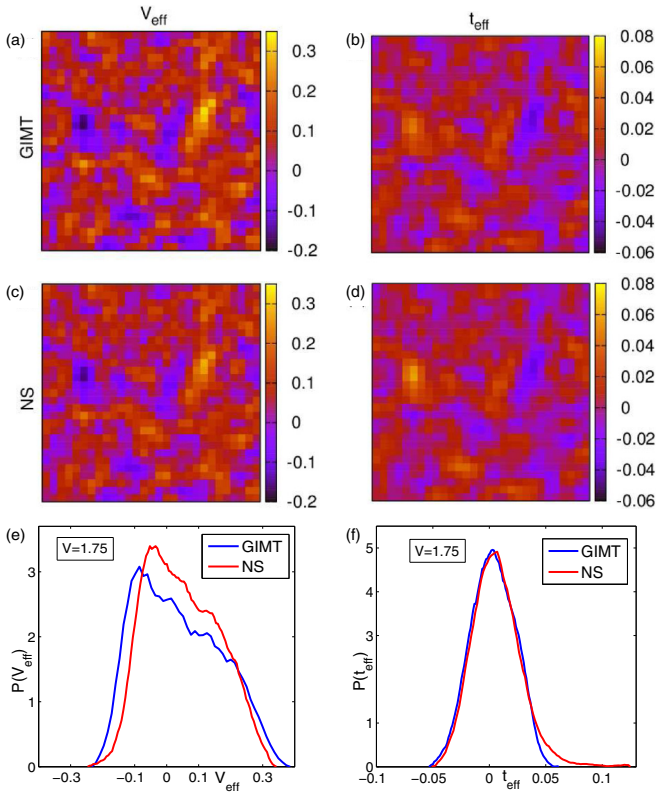

FIG. 1. (a)–(d) Spatial density map of V_{eff} and t_{eff} from NS and GIMT shows similar spatial anticorrelation between V_{eff} and t_{eff}. They also highlight the spatial correlation in V_{eff}. Comparison of distributions $P(V_{\mathrm{eff}})$ in (e) and $P(t_{\mathrm{eff}})$ in (f) for NS and for the full GIMT outputs at $V = 1.75$. The distributions match rather well in the two calculations validating the basis of PNS calculations. We subtracted the homogeneous components of t_{eff} ($t_{\mathrm{eff}}(V = 0) = 0.459$) and V_{eff} ($V_{\mathrm{eff}}(V = 0) = 1.6$), arising from the Fock and Hartree shifts, respectively. The resulting distributions in (e) and (f) feature zero mean—this is broadly true for all V.

local charge imbalance leads to an interesting feedback loop through g^{t}_{ij}, absent in the uncorrelated systems. The low electronic density at i enhances g^{t}_{ij} according to Eq. (5), which in turn enhances the charge fluctuations across site i, leading to a larger effective ρ_i than what would be its value in the absence of the Gutzwiller factors. This leads to a much weaker effective disorder [39,40,76,77] to account for the enhanced ρ_i. In addition to impurity renormalization, the above argument sheds light on the spatial anticorrelations of V_{eff} and t_{eff}. Both these features make $\mathrm{NS_{GIMT}}$ distinct from the plain exact eigenstates. However, in the limit $U \to 0$, the $\mathrm{NS_{GIMT}}$ and exact eigenstates would be identical. How strong is such renormalization of disorder? In order to get a quantitative estimate of the impurity renormalization, we present the scatter plot of V_{eff} against bare V in Fig. 3 from our self-consistent NS-calculations (statistics collected over 10 realizations of disorder). Our results show a simple linear trend: $V_{\mathrm{eff}} \approx \delta V$ for low V, with weak corrections for stronger V. Here, $\delta = (1 - \rho)$ is the average doping. This low-V linearity is consistent with earlier findings from a single-impurity calculation [39]. This is easily comprehended: since $t \to g^{t} t \sim \delta t$, we must rescale V by the same factor for a justified comparison, yielding

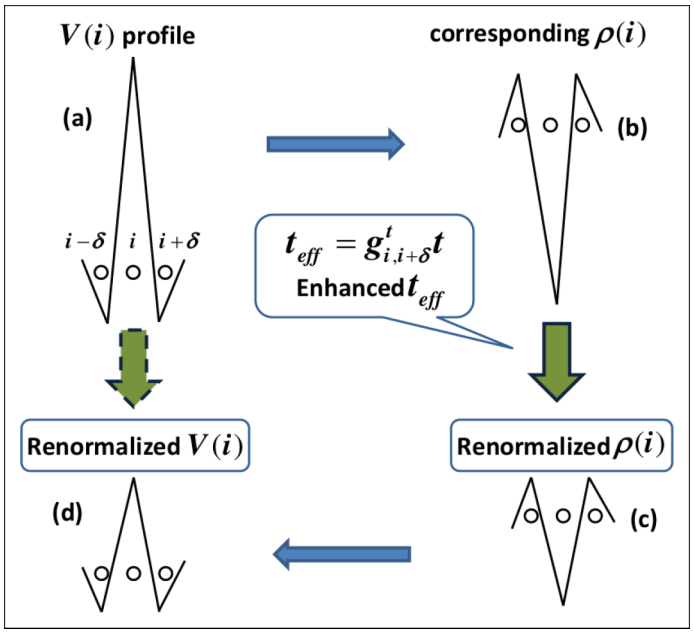

FIG. 2. A schematic evolution of the inhomogeneity in space that leads to the renormalization of $V_{\rm eff}(i)$ and spatial anticorrelation between $V_{\rm eff}(i)$ and $t_{\rm eff}(i)$, upon including electronic repulsions through the Gutzwiller approximation (GA). Consider in (a) the site i having a high hill of disorder potential (also assumed that $V_{i\pm\delta}=0$), that would normally yield a low ρ_i compared to $\rho_{i\pm\delta}\approx\rho_0$, as shown in (b), rarely populating the site i. However, GA insures that $t_{\rm eff}$ on bonds connecting i to its neighbors is enhanced, according to Eq. (5), increasing charge flow to this site. This in turn reduces the dip in ρ_i as seen in (c), so that the corresponding $V_{\rm eff}(i)$, which would have normally produced the ρ_i in (c), is far weaker than its bare value, shown in (a). Exactly similar arguments would yield a similar weakening of deep potential well by strong correlations.

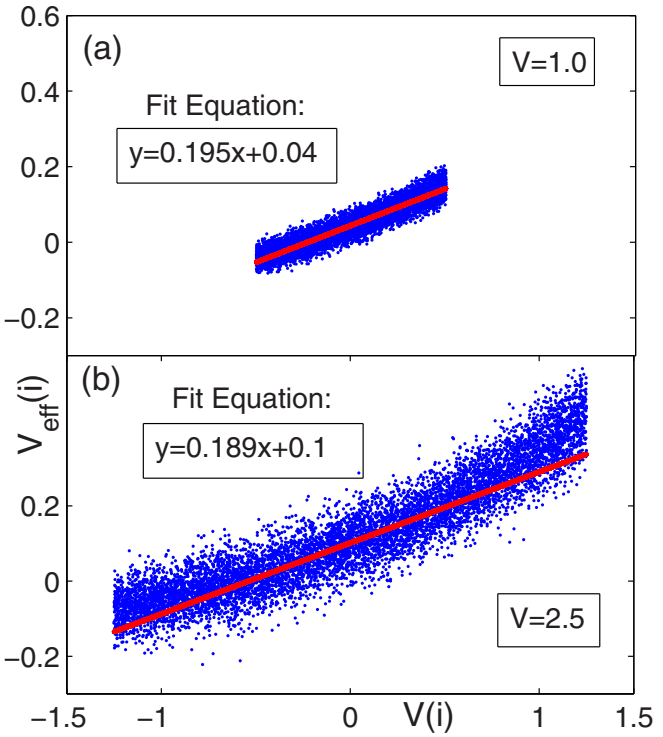

FIG. 3. Scatter plots of $V_{\rm eff}(i)$ against the bare potential $V(i)$ for (a) $V=1.0$ and (b) 2.5. The red lines are the best fit to the data. The slope of the solid line in both panels is close to the average doping ($\delta=0.2$). For $V=2.5$, the data tend to deviate from the fit for larger $|V(i)|$, signaling higher order effects.

$V_{\rm eff}\sim\delta V$. For the cuprate superconductors, we typically have $\delta\leqslant 0.2$. The above considerations then imply that the Fermi's golden rule estimate of the inverse scattering time of the electrons in the underlying $\rm NS_{GIMT}$ is an order of magnitude smaller compared to the "usual" exact eigenstates: $\tau_{\rm NS}^{-1}\sim\tilde{g}(0)V_{\rm eff}^2\sim\delta\tau_0^{-1}$, where $\tilde{g}(0)$ is the density of states at Fermi energy of $\rm NS_{GIMT}$. A similar dependence of τ^{-1} has also been been predicted recently from the T-matrix estimation [42]. We focus next on Cooper pairing between these strongly correlated $\rm NS_{GIMT}$ states.

B. Self-consistent order parameters

Inducing pairing through BCS-type attraction as described in Sec. II C, we find that the self-consistent PNS outputs of the spatial profiles of the pairing amplitude Δ_{ij}, local density ρ_i, or τ_{ij} are nearly indistinguishable from the results of GIMT calculations. In order to quantify the strength of PNS formalism, we find it easier to define the relative difference in the PNS order parameters with respect to those from GIMT, in the following manner:

$$\mathcal{R}_{\rm OP}(i)=\frac{OP^{\rm GIMT}(i)-OP^{\rm PNS}(i)}{\langle OP\rangle^{\rm GIMT}}, \qquad (16)$$

where OP represents either ρ_i, $\Delta_d(i)$, or τ_{ij}. Here, $\langle\rangle$ denotes average over all sites and over configurations. We define the d-wave superconducting order parameter on a site as $\Delta_d(i)=\frac{1}{4}(\Delta_i^{+x}-\Delta_i^{+y}+\Delta_i^{-x}-\Delta_i^{-y})$. We emphasize here that the PNS self-consistency produces for us the solution of link variable Δ_{ij} among other things. This by itself is no confirmation of a d-wave anisotropy of the pairing amplitude. However, our choice of parameters in the Hamiltonian $\mathcal{H}_{t-J}$ ensures that we have *exclusively* the d-wave ($d_{x^2-y^2}$) pairing amplitude in the clean limit. Introduction of disorder does generate other possibilities of bond pairing amplitude, e.g., Δ_{xs}, $\Delta_{s_{xy}}$, and $\Delta_{d_{xy}}$ [78]. But their strengths remain negligibly small compared to the Δ_d component. GIMT calculations also confirm the same qualitative picture in this regard.

We plot the normalized distribution of $\mathcal{R}_{\Delta_d}$ and $\mathcal{R}_\rho$ for different V in Fig. 4. These distributions, always peaked at zero, show only a weak broadening with V. Further, such smearing is essentially independent of V in the range $1.5\leqslant V\leqslant 2.5$. The width of the distribution of $\mathcal{R}$ remains only at about 3% for all order parameters up to $V=2.5$, emphasizing the accuracy of the proposed PNS method to describe the strongly correlated dSC. Not only the spatial profile of any order parameter, from PNS and GIMT calculations, appears nearly indistinguishable [74], more importantly, $\mathcal{R}$ remains strongly correlated in space with the corresponding order parameter profile itself. To illustrate this, we show in the insets of Fig. 4(a) Δ_d (left) and $\mathcal{R}_{\Delta_d}$ (right) in space for $V=2.5$ (for one realization of disorder), and similarly for local densities in

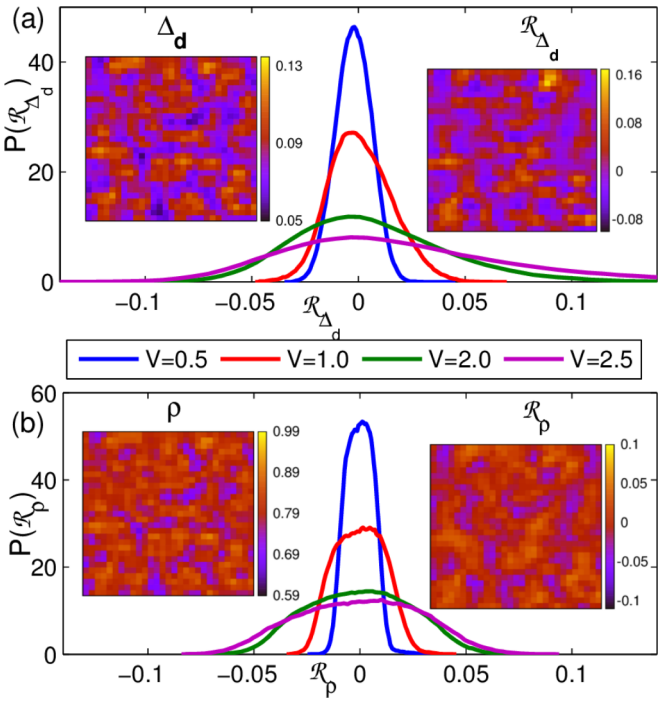

FIG. 4. Main panels: The distribution $P(\mathcal{R}_{\Delta_d})$ in (a) and of $P(\mathcal{R}_\rho)$ in (b) are shown for various disorder strengths. Sharply peaked nature of these distributions (with small variance) validates the PNS formalism. The left inset of panel (a) shows the PNS results for the spatial profile of Δ_d at $V = 2.5$, where as the right inset presents that of $\mathcal{R}_{\Delta_d}$. The strong resemblance of the two ascertains that the small differences between GIMT and PNS outputs are not just random in space, but are highly correlated with the order parameter profile. The insets of panel (b) draw similar inferences as those in (a), but for local densities.

Fig. 4(b). The strong resemblance of the two spatial structures in each panel is evident. Thus, any marginal differences of the order parameters from the two methods at any location is sufficient to reconstruct such differences everywhere in space.

C. Off-diagonal long-range order

In order to illustrate the accuracy of the PNS results for physical observables, we study the V dependence of the superconducting off-diagonal long-range order (ODLRO), defined as

$$\Delta_{\rm OP}^2 = \lim_{|i-j|\to\infty} F_{\delta,\delta'}(i-j), \tag{17}$$

where the pair-pair correlation function, $F_{\delta,\delta'}(i-j) = \langle B_{i\delta}^\dagger B_{j\delta'}\rangle$, and, $B_{i\delta}^\dagger = (c_{i\uparrow}^\dagger c_{i+\delta\downarrow}^\dagger + c_{i+\delta\uparrow}^\dagger c_{i\downarrow}^\dagger)$ is the singlet Cooper-pair creation operator on the links connecting the neighboring sites at i and $i+\delta$. Since $F_{\delta,\delta'}(i-j)$ can be interpreted as simultaneous hopping of a singlet cooper pair on a link, the Gutzwiller factor corresponding to this process becomes $g_{i,j}^t g_{i+\delta,j+\delta'}^t$. We calculate $F_{\delta,\delta'}(i-j)$ using the transformations Eqs. (6) and (12). The value of $\Delta_{\rm OP}$, from the above prescription matches well with $\sum_{\langle ij\rangle} g_{ij}^t \Delta_{ij}$ for all V studied, as expected from the BCS-type treatment in the presence of Hilbert-space projection. The evolution of ODLRO (normalized by its value $\Delta_{\rm OP}^{(0)}$ at $V = 0$) with V, as

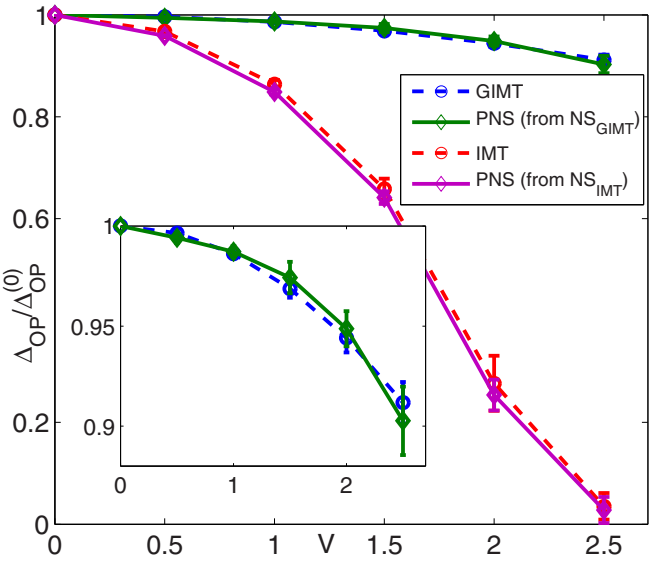

FIG. 5. Evolution of $\Delta_{\rm OP}$ is presented against V. The V dependencies of both the PNS and GIMT results show nearly identical behavior. The inset shows an expanded region of the main panel establishing that the PNS findings match excellently with those from GIMT within the error bars. The results for $\Delta_{\rm OP}$ from IMT calculations, shown by the magenta curve (forcing all Gutzwiller factors to unity, and thereby neglecting strong electronic repulsions), deviate significantly from the PNS or GIMT results. However, it still complements the plain BdG results (red dashed line) exceedingly well.

evaluated from the PNS and GIMT calculations, was discussed briefly in Ref. [74], and we include it here in Fig. 5 for completeness. The main panel shows that the PNS results are nearly identical with the GIMT findings (see the inset for an expanded view), ascertaining that PNS formalism serves as good a purpose as the GIMT method for handling the physics of strong correlations.

An independent test for the effectiveness of the PNS formalism comes from its comparison with a full BdG calculation, when both neglect strong correlations (and will be referred to as IMT, henceforth). Suppression of strong correlations, though unphysical for cuprates, can easily be implemented by setting all Gutzwiller factors to unity. In Fig. 5, we also compared $\Delta_{\rm OP}(V)$ as obtained from pairing between $NS_{\rm IMT}$ with those from corresponding plain BdG outcomes. The excellent match of the two formalisms even in the uncorrelated domain strengthens the PNS method as a natural description of disordered superconductors. Note that the results differ significantly by including and excluding Gutzwiller factors—irrespective of PNS or BdG methods (see also Sec. III F).

D. Density of states

The other hallmark of superconductors is their density of states (DOS), $N(\omega)$, featuring a characteristic gap to single-particle excitations. This gap signifies the gain in the condensation energy as superconductivity sets in, pushing the low-lying normal states (with respect to the chemical potential) to the gap edge and thereby forming coherence peaks. It is well known that the d-wave anisotropy of the pairing amplitude of

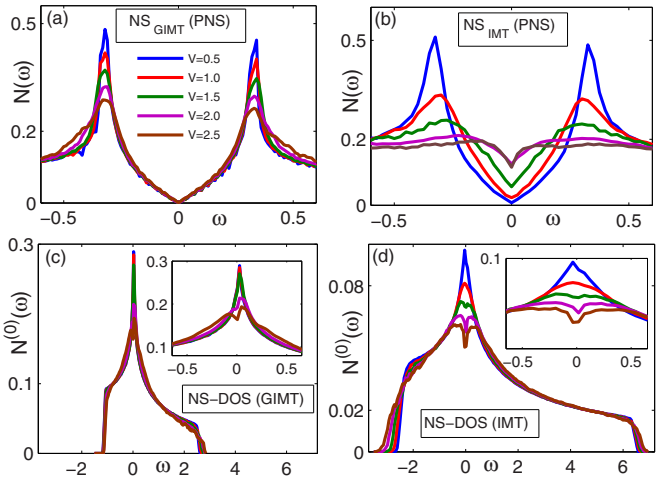

FIG. 6. DOS of dSC state calculated within PNS from (a) NS_{GIMT} and (b) NS_{IMT}. The features in (a) and (b) match very well with the findings of GIMT and IMT, respectively. DOS for the normal states (c) NS_{GIMT} and (d) NS_{IMT}. Insets of (c) and (d) show an expanded view of the DOS at low energies. For $V \geq 0.5$, NS_{IMT} becomes flat near the chemical potential analogous to an Anderson insulator. Strongly correlated NS_{GIMT} preserves the Van Hove singularity owing to the complex interplay of $V_{\rm eff}$ and $t_{\rm eff}$. A soft gap develops at the chemical potential for $V \geq 2.0$ in both NS_{GIMT} and NS_{IMT}.

cuprates produces linear ω dependence of DOS, i.e., $N(\omega) \sim |\omega|$, for small $|\omega|$. Within PNS formalism, DOS is expressed as

$$N(\omega) = \frac{1}{N}\sum_{i,n} g_{ii}^{t}[|u_{i,n}|^2\delta(\omega - E_n) + |v_{i,n}|^2\delta(\omega + E_n)], \tag{18}$$

where $u_{i,n} = \sum_{p=1}^{N}(\psi_i^p)u_{p,n}$ and $v_{i,n} = \sum_{p=1}^{N}(\psi_i^p)v_{p,n}$, and ψ_i^p is given by Eq. (6). Our numerical evaluation of DOS implements repeated zone scheme on a supercell of 12×12 unit cells for a better resolved DOS. Figures 6(a) and 6(b) show the DOS for the dSC state obtained from NS_{GIMT} and NS_{IMT}, respectively. All the features of DOS of the full BdG calculations (using both GIMT and IMT schemes) are captured excellently in the PNS results, as seen by comparing our current PNS results with those in Figs. 3(a) and 3(b) of Ref. [40]. In particular, the presence of strong correlations in NS_{GIMT} make the low-energy $N(\omega)$ robust to disorder up to $V = 2.5$ [see Fig. 6(a)]. On the other hand, PNS results for NS_{IMT} experience gap-filling as V increases, though it remains identical to the corresponding full BdG results. These findings, together with the success of describing the V dependence of $\Delta_{\rm OP}$ in Fig. 5 builds confidence in our simple yet robust pairing description.

However, the PNS method derives deeper insights into the evolution of superconductivity by illustrating the key physics in terms of the underlying DOS of the normal states, $N^{(0)}(\omega) = \sum_n \delta(\omega - E_n^{(0)})$, calculated within the realm of GIMT and IMT respectively, as shown in Figs. 6(c) and 6(d). The IMT results of $N_{\rm IMT}^{(0)}(\omega)$ in Fig. 6(d) are expectedly similar to that of a standard Anderson insulator. The asymmetry in $N_{\rm GIMT}^{(0)}(\omega)$ and $N_{\rm IMT}^{(0)}(\omega)$ about $\omega = 0$ is largely due to the inclusion of the next-nearest neighbor hopping in our $\mathcal{H}_{\rm NS}$, and partly due to our choice of $\rho = 0.8$ (away from half-filling). Both of these profiles of NS-DOS feature a Van Hove singularity at $\omega = 0$ in the clean case. However, the restrictions of phase space for allowed hopping in NS_{GIMT}, owing to the strong electronic repulsions, reduces the bandwidth significantly and therefore increases the magnitude of $N_{\rm GIMT}^{(0)}(\omega)$, as the total number of states in the band must be conserved.

The nature of the suppression of the Van Hove singularity in DOS with disorder, on the other hand, shows sharp contrast in the IMT and GIMT calculations. We find that with increasing V the $N_{\rm IMT}^{(0)}(\omega)$ (which is much smaller in magnitude near $\omega \sim 0$, compared to the GIMT counterpart) becomes increasingly flat over a wide range of ω around the chemical potential, resembling an Anderson insulator. The corresponding $N_{\rm GIMT}^{(0)}(\omega)$, on the other hand, shows a rather weak evolution with V, preserving a large weight close to $\omega \sim 0$. We next integrate these findings with our earlier conclusions that the low-lying NS_{GIMT} remains largely delocalized for up to $V \approx 2$, whereas NS_{IMT} becomes strongly localized well within the system [79]. As a result, it becomes harder for pairing attraction to form Cooper pairs and establish superconductivity from these localized Anderson-insulating IMT normal states near $\omega \sim 0$. This naturally fills up the superconducting gap. On the other hand, the delocalized nature of low-lying NS_{GIMT} and their large weight in DOS near $\omega = 0$, even for $V = 2.5$, remain conducive to establishing a healthy dSC, with a nearly V-independent $N(\omega)$ for low ω.

Finally, we draw attention to the intriguing emergence of a tiny gaplike feature at $\omega = 0$ in both $N_{\rm GIMT}^{(0)}(\omega)$ and $N_{\rm IMT}^{(0)}(\omega)$ for $V \approx 2.5$ [see the insets of Figs. 6(c) and 6(d)]. Hubbard repulsions are found to open up a narrow gap in disordered systems [80–83], whose energy scale relates to hopping strength. The incipient thin gap in our results for $V \approx 2.5$ is qualitatively consistent with Refs. [82,83], and a detailed understanding and significance of such a gap will be addressed elsewhere. But this naturally prompts us to limit the applicability of PNS formalism to larger disorder strengths, as a gap in the NS-DOS goes against a simple pairing theory like ours. Moreover, strong disorder has other intricacies [48] demanding higher-order refinements to our pairing description.

E. Pairing of limited states with close by energies

As discussed in Sec. II C, the PNS method amounts to pairing between all the eigenstates of $\mathcal{H}_{\rm NS}$, making its numerical implementation computationally as demanding as that of GIMT. However, technical gain can be insured by having to pair only a limited number of normal states α and β that are not too far from the Fermi energy, such that, $\xi_\alpha \approx \xi_\beta$. Such an expectation is, of course, motivated by the structure of the BCS gap equation.

In search of this simplification, we plot in Figs. 7(a) and 7(b), the fully self-consistent and disorder averaged profiles of $|\Delta_{\alpha\beta}|$ in the eigenspace of α and β. The near diagonal structures of $|\Delta_{\alpha\beta}|$ implies that the states α, β which are far in energies, have negligible contributions in $\Delta_{\alpha\beta}$. Such a diagonal character of $\Delta_{\alpha\beta}$ is well maintained for $V \leqslant 3$.

The diagonal nature is preserved when the same $|\Delta_{\alpha\beta}|$ is plotted against ξ_α and ξ_β [shown for $V = 2.5$ in Fig. 7(c)]. We also note that not all normal states contribute to "diagonal"

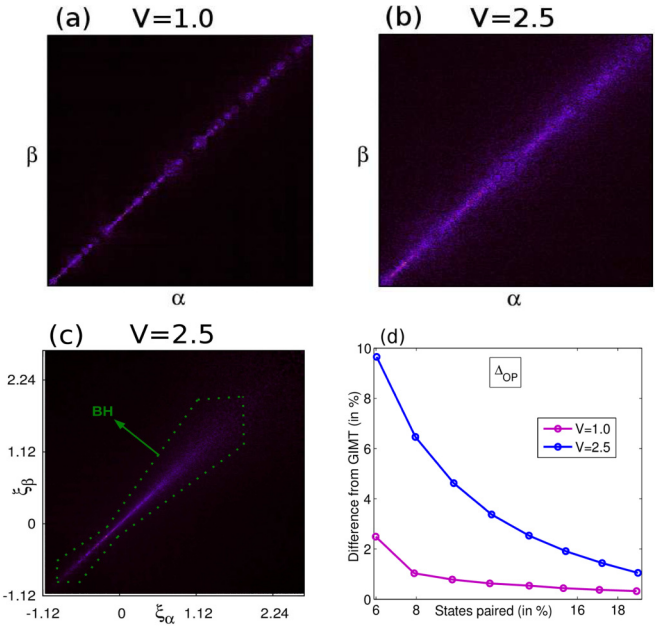

FIG. 7. Intensity plot of $|\Delta_{\alpha\beta}|$ in the normal state eigenbasis α-β for (a) $V = 1.0$ and (b) 2.5. We show $|\Delta_{\alpha\beta}|$ in a limited range of α,β (only the central part) for a better resolution. The presented values of $|\Delta_{\alpha\beta}|$ are scaled by their maximum values for clarity (0.35 for $V = 1.0$ and 0.3 for $V = 2.5$). The near-diagonal nature of the pairing is evident for both V. The color scales are identical to that in Fig. 1. (c) Density plot of $|\Delta_{\alpha\beta}|$ against ξ_α and ξ_β across the full (renormalized) bandwidth for $V = 2.5$. While the diagonal character of $|\Delta_{\alpha\beta}|$ is evident, only negligible contribution to $|\Delta_{\alpha\alpha}|$ comes from the states near band edges. (d) Accuracy of PNS (with respect to GIMT) is shown along y axis, against the percentage of states paired (along x axis). This accuracy, already impressive with about 10% NS_{GIMT} participating in pairing, becomes better as more states included in Cooper pairing.

pairing, particularly those states lying close to band edges contribute only negligibly to $|\Delta_{\alpha\alpha}|$. Such contribution would have been limited only to a narrow energy window, $\pm\hbar\omega_D$, in simple BCS theory (ω_D being the Debye frequency). In the present case of strongly correlated anisotropic superconductors in the presence of disorder, the energy range of contribution is wider. The asymmetry of the states about the Fermi energy ($\xi = 0$) in GIMT energy band in Fig. 7(c) reflects the same imbalance of $N^{(0)}_{GIMT}(\omega)$ of Fig. 6(c). The final profile of $|\Delta_{\alpha\beta}|$, as seen from Fig. 7(c), hints that the summations in Eqs. (13) and (14) can be further restricted to a limited set (leaving out the states close to band edges) to achieve a desired accuracy.

Motivated by these findings, we simplify the PNS calculations by limiting progressively the smaller number of total states contributing to pairing. The corresponding output of Δ_{OP}, as its percentage deviation from the GIMT value, is shown in Fig. 7(d) against the fraction of normal states participated in pairing. To illustrate our choice of restricted states for $V = 2.5$, we show the bounding box BH in Fig. 7(c) by a thin dotted line that includes about 19% of the normal states for pairing, and results into more than 99% accuracy in Δ_{OP} [the last data point along x axis in Fig. 7(d)]. It is apparent that our bounding box encloses states that subscribe to $|\Delta_{\alpha\beta}|$ of significance [84]. Evidently, PNS results achieve perfection when increasing fraction of states are included. Yet, we see that only about 10% of NS_{GIMT} ensures 95% accuracy of the results, even for disorder as large as $V = 2.5$!

F. Pairing theory with "uncorrelated" NS and with a different model of disorder

We discuss below the prospects of our PNS proposal in terms of "uncorrelated" normal states, in which all Gutzwiller factors are set to unity. The impressive match of Δ_{OP} from such pairing theory using NS_{IMT}, in comparison with the plain BdG results, has already been analyzed in Sec. III C. In fact, we found that the IMT-normal states are very close to the original exact eigenstates, except, of course, for the Hartree and Fock shifts, which add only weak corrections in the absence of Gutzwiler renormalization. While the success of PNS formalism is evident, there are practical concerns for the applicability of such implementation. The NS_{IMT} are naturally incapable of accounting for the strong correlation effects, crucial for the qualitative physics of the strongly correlated superconductors. In addition, the pairing of NS_{IMT} misses the near-diagonal nature of $|\Delta_{\alpha\beta}|$ as found in Fig. 7 for NS_{GIMT}, making the NS_{IMT} less useful, for deriving technical advantages over IMT calculations, as discussed in Ref. [74].

We also verified that the results and conclusions of PNS formalism remain valid even with a model of concentration impurity, in which n_{imp} fraction of the (random) lattice sites contain a fixed disorder potential V_0, provided we use $V_0 \leqslant 3$. Stronger V_0 brings in subtle effects even in GIMT implementation [48].

IV. DISCUSSIONS

The impressive match between the PNS and GIMT results is inspiring from the perspective of developing simple understanding on the complex physics of disordered and strongly correlated superconductors. However, we believe that it is the conceptual advances offered by PNS technique, as described in the previous sections, which have far reaching values. We will discuss below a crucial notional gains from the PNS proposal.

A. Insensitivity of inhomogeneity in pairing

Our results make it evident that inhomogeneities are less relevant for pairing in case of strongly correlated dSC. This has already been illustrated in Ref. [40], by matching the spectral density of states evaluated in GIMT for $V \leqslant 3t$, with its d-wave BCS form convoluted with the near-Gaussian GIMT distribution of Δ_{ij}. Here, we argue for a more direct evidence to this assertion by noting that the spatial inhomogeneities in the Gutzwiller factor g^{xy}_{ij}, arising from the spatial fluctuations in the local density, has little role in the final self-consistent output of Δ_{ij} on the bonds. This is, however, only true, provided that the *correct* NS_{GIMT} is obtained by taking care of all inhomogeneities in their construction. For concreteness, we can consider three independent implementations of g^{xy}_{ij}, with a progressive degree of approximations of the inhomogeneities: (a) a full self-consistency in local density ρ_i in the definition of g^{xy}_{ij} is achieved during the iterative update of Δ_{ij} during the pairing stage following Eq. (8). (b) We fix the inhomogeneous

density profile to its form as obtained in NS_{GIMT}, without any update during the pairing self-consistency. (c) In the extreme approximation, we set $g_{ij}^{xy} = (1 - 0.5\rho)^{-2}$ for the purpose of pairing self-consistency. Obviously, each degree of approximation is associated with significant computational gains. We find that even with the most drastic approximation, the resulting order parameters are in good agreement (within 10%) with the GIMT findings. On the other hand, we found that an approximate handling of heterogeneities in the normal state leads to significant deviation of the final results.

B. What makes d-wave anisotropy of pairing so robust?

Why does not AG-theory capture the insensitivity of strongly correlated d-wave superconductors to impurities? Admittedly, such strongly coupled systems with short coherence length ξ, in addition to spatially fluctuating pairing amplitude in response to disorder, fall outside the scope of a true AG description. However, strong correlations have recently been incorporated within a self-consistent T-matrix calculation [76], and found a resulting weakening of the pair-breaking mechanism [42]. While such a description still makes homogeneous approximation of the disordered medium, we show here that the true role of disorder in the presence of strong electronic repulsion is more subtle. As substantiated in Figs. 1 and 2, that even though the bare disorder describe only the on-site random potential, the normal state quasiparticles experience an emerging disorder in the hopping as well. In fact, the immunity of strongly correlated superconductors to impurity presents a classic example of "order by disorder," where spatially anticorrelated nature of t_{eff} and V_{eff} weakens the overall disorder in the system far more, even though the individual (renormalized) components are not that weak. A study of the normal states, thus, illustrates how the charge inhomogeneities are spatially smeared out due to the repulsive interactions within a quasiparticle description.

Moreover, our PNS formalism offers a simple and intuitive perspective for the distinct outcome of the GIMT findings. Such results (or the results from PNS, which produces essentially identical results as GIMT) of the spatial profile of Δ_{ij} on each bond on a square lattice is shown in Fig. 8(a), for a specific realization of disorder.

We witness pairing amplitudes of opposite signs but of nearly equal strengths on bonds along $\hat{x}$ and $\hat{y}$ directions from each site for $V = 2.5$ [see Fig. 8(a)]. Such a phase differences of $\pi/2$ between adjacent orthogonal bonds is the hallmark of its $d_{x^2-y^2}$ anisotropy of pairing amplitude [23–25] in the clean systems, and remains near-perfect even at $V = 2.5$! With the introduction of disorder, AG theory predicts that the impurity scattering "mixes-up" such sensitive phase relations, and thereby depletes d-wave superconductivity [6]. Instead, we find a healthy d-wave anisotropy to survive. But, this is naturally expected within the PNS formalism—there is no disorder left to scramble phases at the second stage of "pairing," they are all consumed in generating the normal states at the first stage of calculations!

Do such phase relations continue to hold for stronger disorders? While additional considerations are necessary for pushing the applicability of the PNS method to larger V, an extension of GIMT-type calculation upon including localization physics for $V \geqslant 3$ has already been reported in Ref. [48], and those results offer a significant pointer. By ramping up V in such calculations, we find that for $V = 4.5$, the local pairing amplitude tends to zero identically on *both* $\hat{x}$ and $\hat{y}$ bonds in regions of strong fluctuation of disorder potential [marked by circular boundary in Fig. 8(b)]. Yet, the d-wave anisotropy remains intact in regions possessing a healthy Δ_{ij} (marked by square boundary), albeit some inhomogeneity. Thus, impurities can affect superconductivity by locally collapsing the self-consistent pairing amplitudes, which are due to the localization properties of the normal states, but are not because of scrambling of the d-wave anisotropy.

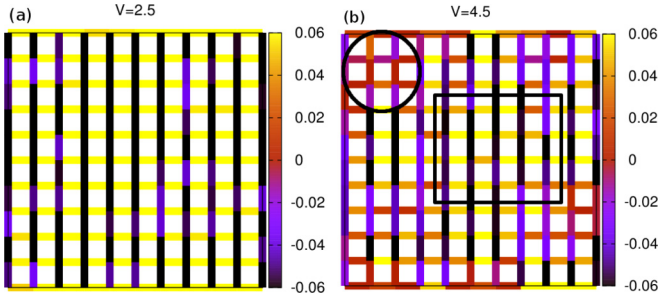

FIG. 8. Δ_{ij} on each bond for a section of the lattice for (a) $V = 2.5$ and (b) 4.5 for a specific realization of disorder. The $\pi/2$ phase difference between $\Delta_{i,i+\hat{x}}$ and $\Delta_{i,i+\hat{y}}$ survives over the entire lattice as seen in (a). The larger disorder strength of (b) still supports the d-wave anisotropy in most parts (highlighted by the square boundary). It also features regions of strong potential fluctuations (marked by circular boundary), where $\Delta_{i,i+\hat{x}}$ and $\Delta_{i,i+\hat{y}}$ are closer in magnitude, but only when both are vanishingly small!

V. CONCLUSION

In conclusion, we presented a description of disordered and strongly correlated d-wave superconductors by implementing simple pairing ideas of Anderson, but extending it by including the effects of strong electronic correlations as well as disorder induced inhomogeneities. The impressive match of the results from the proposed PNS method and GIMT findings is encouraging. In addition to offering a deeper understanding of the GIMT findings, our formalism sheds important light on some shortcomings of the conventional wisdom. The pivotal advance offered by the PNS formalism lies in identifying the underlying exact quasiparticle states of these strongly correlated materials that participate in Cooper pairing in unconventional superconductors. This motivates future survey of the properties of NS_{GIMT} by probing them using various means, and in particular on their temperature dependences. It will also be interesting to consider the robustness of the PNS formalism upon including the physics of "competing orders" in NS_{GIMT} and their role in subsequent Cooper pairing.

ACKNOWLEDGMENTS

We thank I. Paul and K. Miyake for useful discussions. D.C. acknowledges fellowship from the Council of Scientific and Industrial Research (CSIR), India.

[1] H. Alloul, J. Bobroff, M. Gabay, and P. J. Hirschfeld, Rev. Mod. Phys. **81**, 45 (2009).
[2] E. Dagotto, Science **309**, 257 (2005).
[3] B. Keimer, S. A. Kivelson, M. R. Norman, S. Uchida, and J. Zaanen, Nature **518**, 179 (2015).
[4] B. Nachumi, A. Keren, K. Kojima, M. Larkin, G. M. Luke, J. Merrin, O. Tchernyshöv, Y. J. Uemura, N. Ichikawa, M. Goto *et al.*, Phys. Rev. Lett. **77**, 5421 (1996).
[5] A. Garg, M. Randeria, and N. Trivedi, Nat. Phys. **4**, 762 (2008).
[6] A. Abrikosov and L. Gorkov, Sov. Phys. JETP **12**, 1243 (1961).
[7] P. Hirschfeld, D. Vollhardt, and P. Wölfle, Solid State Commun. **59**, 111 (1986).
[8] S. Schmitt-Rink, K. Miyake, and C. M. Varma, Phys. Rev. Lett. **57**, 2575 (1986).
[9] R. Joynt, J. Low Temp. Phys. **109**, 811 (1997).
[10] N. E. Hussey, Adv. Phys. **51**, 1685 (2002).
[11] A. V. Balatsky, I. Vekhter, and J.-X. Zhu, Rev. Mod. Phys. **78**, 373 (2006).
[12] C. Pépin and P. A. Lee, Phys. Rev. B **63**, 054502 (2001).
[13] H. Won, K. Maki, and E. Puchkaryov, *Introduction to D-Wave Superconductivity* (Springer Netherlands, Dordrecht, 2001), pp. 375–386.
[14] J. A. Slezak, J. Lee, M. Wang, K. McElroy, K. Fujita, B. M. Andersen, P. J. Hirschfeld, H. Eisaki, S. Uchida, and J. C. Davis, Proc. Natl. Acad. Sci. **105**, 3203 (2008).
[15] K. McElroy, D.-H. Lee, J. E. Hoffman, K. M. Lang, J. Lee, E. W. Hudson, H. Eisaki, S. Uchida, and J. C. Davis, Phys. Rev. Lett. **94**, 197005 (2005).
[16] S. H. Pan, J. P. O'Neal, R. L. Badzey, C. Chamon, H. Ding, J. R. Engelbrecht, Z. Wang, H. Eisaki, S. Uchida, A. K. Gupta *et al.*, Nature **413**, 282 (2001).
[17] K. M. Lang, V. Madhavan, J. E. Hoffman, E. W. Hudson, H. Eisaki, S. Uchida, and J. C. Davis, Nature **415**, 412 (2002).
[18] P. W. Anderson, Science **288**, 480 (2000).
[19] A. F. Kemper, D. G. S. P. Doluweera, T. A. Maier, M. Jarrell, P. J. Hirschfeld, and H.-P. Cheng, Phys. Rev. B **79**, 104502 (2009).
[20] F. Rullier-Albenque, H. Alloul, and R. Tourbot, Phys. Rev. Lett. **91**, 047001 (2003).
[21] S. K. Tolpygo, J.-Y. Lin, M. Gurvitch, S. Y. Hou, and J. M. Phillips, Phys. Rev. B **53**, 12454 (1996).
[22] D. A. Wollman, D. J. Van Harlingen, J. Giapintzakis, and D. M. Ginsberg, Phys. Rev. Lett. **74**, 797 (1995).
[23] D. A. Wollman, D. J. Van Harlingen, W. C. Lee, D. M. Ginsberg, and A. J. Leggett, Phys. Rev. Lett. **71**, 2134 (1993).
[24] H. Ding, M. R. Norman, J. C. Campuzano, M. Randeria, A. F. Bellman, T. Yokoya, T. Takahashi, T. Mochiku, and K. Kadowaki, Phys. Rev. B **54**, R9678 (1996).
[25] C. C. Tsuei, J. R. Kirtley, C. C. Chi, Lock See Yu-Jahnes, A. Gupta, T. Shaw, J. Z. Sun, and M. B. Ketchen, Phys. Rev. Lett. **73**, 593 (1994).
[26] J. G. Analytis, A. Ardavan, S. J. Blundell, R. L. Owen, E. F. Garman, C. Jeynes, and B. J. Powell, Phys. Rev. Lett. **96**, 177002 (2006).
[27] J. Li, Y. F. Guo, S. B. Zhang, J. Yuan, Y. Tsujimoto, X. Wang, C. I. Sathish, Y. Sun, S. Yu, W. Yi *et al.*, Phys. Rev. B **85**, 214509 (2012).
[28] M. N. Gastiasoro, F. Bernardini, and B. M. Andersen, Phys. Rev. Lett. **117**, 257002 (2016).
[29] Y. K. Kuo, C. W. Schneider, M. J. Skove, M. V. Nevitt, G. X. Tessema, and J. J. McGee, Phys. Rev. B **56**, 6201 (1997).
[30] E. Dagotto, Rev. Mod. Phys. **66**, 763 (1994).
[31] P. W. Anderson, P. A. Lee, M. Randeria, T. M. Rice, N. Trivedi, and F. C. Zhang, J. Phys.: Condens. Matter **16**, R755 (2004).
[32] P. A. Lee, N. Nagaosa, and X.-G. Wen, Rev. Mod. Phys. **78**, 17 (2006).
[33] W. A. Atkinson, P. J. Hirschfeld, and A. H. MacDonald, Phys. Rev. Lett. **85**, 3922 (2000).
[34] A. Ghosal, M. Randeria, and N. Trivedi, Phys. Rev. B **63**, 020505 (2000).
[35] W. Atkinson, P. Hirschfeld, and A. MacDonald, Physica C **341-348**, 1687 (2000).
[36] M. Franz, C. Kallin, A. J. Berlinsky, and M. I. Salkola, Phys. Rev. B **56**, 7882 (1997).
[37] F. C. Zhang, C. Gros, T. M. Rice, and H. Shiba, Supercond. Sci. Technol. **1**, 36 (1988).
[38] R. B. Christensen, P. J. Hirschfeld, and B. M. Andersen, Phys. Rev. B **84**, 184511 (2011).
[39] N. Fukushima, C.-P. Chou, and T. K. Lee, Phys. Rev. B **79**, 184510 (2009).
[40] D. Chakraborty and A. Ghosal, New J. Phys. **16**, 103018 (2014).
[41] B. M. Andersen and P. J. Hirschfeld, Phys. Rev. Lett. **100**, 257003 (2008).
[42] S. Tang, V. Dobrosavljević, and E. Miranda, Phys. Rev. B **93**, 195109 (2016).
[43] P. Anderson, J. Phys. Chem. Solids **11**, 26 (1959).
[44] A. Ghosal, M. Randeria, and N. Trivedi, Phys. Rev. B **65**, 014501 (2001).
[45] K. Tanaka and F. Marsiglio, Phys. Rev. B **62**, 5345 (2000).
[46] A. V. Balatsky, M. I. Salkola, and A. Rosengren, Phys. Rev. B **51**, 15547 (1995).
[47] A. Kreisel, P. Choubey, T. Berlijn, W. Ku, B. M. Andersen, and P. J. Hirschfeld, Phys. Rev. Lett. **114**, 217002 (2015).
[48] D. Chakraborty, R. Sensarma, and A. Ghosal, Phys. Rev. B **95**, 014516 (2017).
[49] J. Bardeen, L. N. Cooper, and J. R. Schrieffer, Phys. Rev. **106**, 162 (1957).
[50] P. W. Anderson, Science **235**, 1196 (1987).
[51] J. Spałek, Acta Phys. Pol. A **111**, 409 (2007).
[52] J. Hubbard, Proc. R. Soc. London A **276**, 238 (1963).
[53] K. A. Chao, J. Spalek, and A. M. Oles, J. Phys. C **10**, L271 (1977).
[54] J. Spałek, Phys. Rev. B **37**, 533 (1988).
[55] M. M. Maśka, Ż. Śledź, K. Czajka, and M. Mierzejewski, Phys. Rev. Lett. **99**, 147006 (2007).
[56] A. Samanta and R. Sensarma, Phys. Rev. B **94**, 224517 (2016).
[57] M. R. Norman, M. Randeria, H. Ding, and J. C. Campuzano, Phys. Rev. B **52**, 615 (1995).
[58] V. J. Emery, S. A. Kivelson, and J. M. Tranquada, Proc. Natl. Acad. Sci. **96**, 8814 (1999).
[59] E. Fradkin, S. A. Kivelson, M. J. Lawler, J. P. Eisenstein, and A. P. Mackenzie, Ann. Rev. Condens. Matter Phys. **1**, 153 (2010).
[60] E. G. Moon and S. Sachdev, Phys. Rev. B **80**, 035117 (2009).
[61] A. Mesaros, K. Fujita, S. D. Edkins, M. H. Hamidian, H. Eisaki, S.-i. Uchida, J. C. S. Davis, M. J. Lawler, and E.-A. Kim, Proc. Natl. Acad. Sci. **113**, 12661 (2016).
[62] J. P. L. Faye and D. Sénéchal, Phys. Rev. B **95**, 115127 (2017).
[63] B. M. Andersen, P. J. Hirschfeld, A. P. Kampf, and M. Schmid, Phys. Rev. Lett. **99**, 147002 (2007).
[64] E. Fradkin, S. A. Kivelson, and J. M. Tranquada, Rev. Mod. Phys. **87**, 457 (2015).

[65] X. Montiel, T. Kloss, and C. Pépin, Phys. Rev. B **95**, 104510 (2017).
[66] S. Chakravarty, R. B. Laughlin, D. K. Morr, and C. Nayak, Phys. Rev. B **63**, 094503 (2001).
[67] C. M. Varma, Phys. Rev. B **55**, 14554 (1997).
[68] B. Fauqué, Y. Sidis, V. Hinkov, S. Pailhès, C. T. Lin, X. Chaud, and P. Bourges, Phys. Rev. Lett. **96**, 197001 (2006).
[69] B. Edegger, V. N. Muthukumar, and C. Gros, Adv. Phys. **56**, 927 (2007).
[70] W.-H. Ko, C. P. Nave, and P. A. Lee, Phys. Rev. B **76**, 245113 (2007).
[71] A. Paramekanti, M. Randeria, and N. Trivedi, Phys. Rev. B **70**, 054504 (2004).
[72] R. Sensarma, M. Randeria, and N. Trivedi, Phys. Rev. Lett. **98**, 027004 (2007).
[73] J. Spałek, M. Zegrodnik, and J. Kaczmarczyk, Phys. Rev. B **95**, 024506 (2017).
[74] A. Ghosal, D. Chakraborty, and N. Kaushal, Physica B (2017), doi:10.1016/j.physb.2017.08.040.
[75] D. D. Johnson, Phys. Rev. B **38**, 12807 (1988).
[76] S. Tang, E. Miranda, and V. Dobrosavljevic, Phys. Rev. B **91**, 020501 (2015).
[77] D. Tanaskovic, V. Dobrosavljević, E. Abrahams, and G. Kotliar, Phys. Rev. Lett. **91**, 066603 (2003).
[78] K. Seo, B. A. Bernevig, and J. Hu, Phys. Rev. Lett. **101**, 206404 (2008).
[79] See Fig. (8c) and associated discussions in Sec. (3.5) of Ref. [40].
[80] B. Altshuler and A. Aronov, Solid State Commun. **30**, 115 (1979).
[81] A. L. Efros and B. I. Shklovskii, J. Phys. C **8**, L49 (1975).
[82] S. Chiesa, P. B. Chakraborty, W. E. Pickett, and R. T. Scalettar, Phys. Rev. Lett. **101**, 086401 (2008).
[83] H.-Y. Chen, W. A. Atkinson, and R. Wortis, Phys. Rev. B **85**, 235139 (2012).
[84] Accuracy of results could be enhanced by fine tuning our choice of bounding box, but we primarily focused on a simple and robust scheme.